Quarterly Report
Massachusetts Institute of Technology
GAGE Facility GPS Data Analysis Center Coordinator

Thomas Herring and Mike Floyd

Period: 2025/01/01-2025/03/31

Table of Contents

Summary

Under the GAGE2 Facility Data Analysis sub-award, MIT has been processing SINEX files from Central Washington University (CWU) and aligning them to the GAGE NAM14 reference frame. In this report, we show analyses of the data processing for the period 2025/01/01 to 2025/03/31, as well as time series velocity field analyses for the GAGE reprocessing analyses (1996-2025). Several earthquakes were investigated this quarter up to 2025/03/15, and only one of them generated any detectable co-seismic offsets. This earthquake affected only five sites significantly.

Analysis files (pbo format velocity files and offset files) are generated monthly and sent via Python in the middle of each month.

We continue to process ANET data. These solutions are in the ANT14 frame as defined in the ITRF2014 plate motion model [*Altamimi et al.,* 2017].

GPS Analysis of Level 2a and 2b products

Level 2a products: Rapid products

Final and rapid level 2a products have been, in general, generated routinely during this quarter for the CWU solutions. The description of these products, the delivery schedule, and the delivery list remain unchanged from the previous quarter and will not be reported here.

Level 2a products: Final products

The final products are generated weekly and are based on the final JPL orbits and clocks. Finals and rapid solutions are now being generated in the IGS14 system. In this quarter, 1984 stations were processed, 30 fewer than last quarter. In addition, up to 39 sites were processed in the ANET solutions, one more than last quarter. The number of stations processed fluctuated as data systems were updated at EarthScope.

Level 2a products: 12-week, 26-week supplement products

Each week, we also process the Supplemental (12-week latency) and six-month supplemental (26-week latency) analyses from CWU for the main GAGE2

Networks of the Americas stations (NOTA). The delivery schedule for these products is also unchanged.

Analysis of Final products: December 15, 2024–March 22, 2025

For this report, we generated the statistics using the ~3 months of CWU results between December 15, 2024, and March 22, 2025. These results are summarized in Table 1 and Figure 1.

For the three months of the final position time series generated, we fit linear trends and annual signals and compute the RMS scatters of the position residuals in north, east, and up for each station in the analysis. Table 1 shows the median (50%), 70%, and 95% limits for the RMS scatters CWU. The detailed histograms of the RMS scatters are shown in Figure 1 CWU.

Table 1: Statistics of the fits of 1984 stations for CWU analyzed in the finals analysis between December 15, 2024, and March 22, 2025.
Figure 1 shows histograms of the RMS scatters.

Center	North (mm)	East (mm)	Up (mm)
Median (50%)			
CWU	0.85	0.85	4.83
70%			
CWU	1.09	1.08	5.59
95%			
CWU	2.32	2.65	10.70

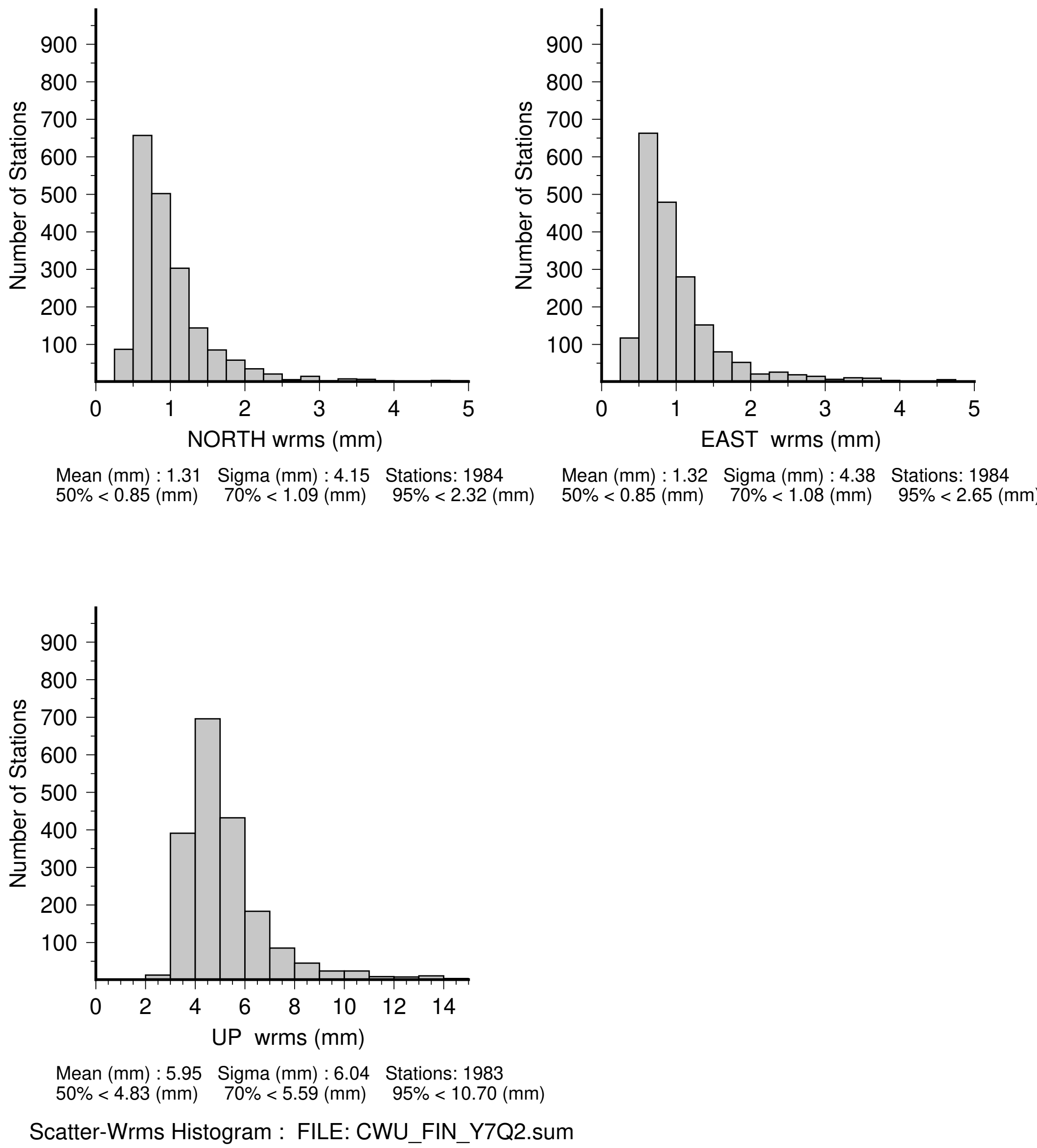

Figure 1: CWU solution histograms of the North, East, and Up RMS scatters of the position residuals for 1984 stations analyzed between December 15, 2024 and March 22, 2025. Linear trends and annual signals were estimated from the time series.

For the CWU analysis, we also evaluate the RMS scatters of the position estimates by network type. The figures below are based on our monthly submissions, but here, we use nominally three months of data to evaluate the RMS scatters. In Table 2, we give the median, 70, and 95 percentile limits on the RMS scatters. The geographical distributions of the RMS scatters by network type are shown in Figures 2-7. The values plotted are given in

CWU_FIN_Y7Q2.tab. There are 1984 stations in the file for sites with at least two measurements during the month.

Table 2: Head and tail of WRMS scatter summary file CWU_FIN_Y7Q1.tab.

```
Tabular Position RMS scatters created from CWU_FIN_Y7Q2.sum
ChiN/E/U are square root of chisquared degree of freedom of the fits.
Values of ChiN/E/U near unity indicate that the estimated error
bars are consistent the scatter of the position estimates

.Site     #    N (mm)  ChiN     E (mm) ChiE    U (mm)  ChiU      Years
 1LSU    26      0.9   0.48      1.3   0.66      5.4   0.61      21.74
 1NSU    33      0.9   0.56      1.0   0.63      6.0   0.83      20.99
 1ULM    33      0.8   0.47      1.2   0.76      5.5   0.76      21.59
 7ODM    97      1.0   0.60      0.7   0.47      4.6   0.68      23.92
…
 ZDV1    94      1.0   0.57      1.0   0.73      5.5   0.88      21.80
 ZKC1    94      1.4   0.83      1.5   1.04      6.4   1.02      21.80
 ZLA1    32      0.8   0.47      0.9   0.60      3.5   0.48      21.62
 ZLC1    32      0.6   0.32      0.5   0.35      4.6   0.64      21.85
 ZME1    32      0.7   0.38      0.9   0.60      5.2   0.73      21.85
 ZMP1    32      0.6   0.32      0.8   0.51      6.5   0.93      22.09
 ZNY1    32      0.7   0.37      0.8   0.53      4.5   0.64      22.01
 ZOA1    91      0.6   0.36      0.5   0.39      4.6   0.73      22.72
 ZSE1    94      0.8   0.42      0.7   0.52      5.6   0.92      22.18
 ZTL4    32      1.2   0.75      0.8   0.51      9.8   1.38      22.20
```

Table 2: RMS scatter of the position residuals for the CWU solution between December 15, 2024, and March 22, 2025, divided by network type. The division of networks is based on the JAVA script unavcoMetdata.jar with network codes PBO, Nucleus, Mid- SCIGN_USGS, America GAMA, COCONet and Expanded PBO

Network	North (mm)	East (mm)	Up (mm)	#Sites
Median				
PBO	0.80	0.81	4.66	806
NUCLEUS	0.74	0.68	4.18	188
GAMA	0.64	0.81	5.29	14
COCONet	1.27	1.29	5.68	70
USGS_SCIGN	0.84	0.76	4.12	123
Expanded	0.92	0.90	5.28	783
70%				
PBO	1.05	1.04	5.21	
NUCLEUS	0.87	0.83	4.82	
GAMA	0.71	0.85	5.55	

COCONet	1.44	1.47	6.15
USGS_SCIGN	1.08	0.96	4.59
Expanded	1.14	1.14	6.08
95%			
PBO	2.49	2.67	9.70
NUCLEUS	1.45	1.55	7.34
GAMA	1.04	0.95	6.05
COCONet	2.88	5.20	11.59
USGS_SCIGN	1.80	1.54	8.22
Expanded	2.41	2.78	12.34

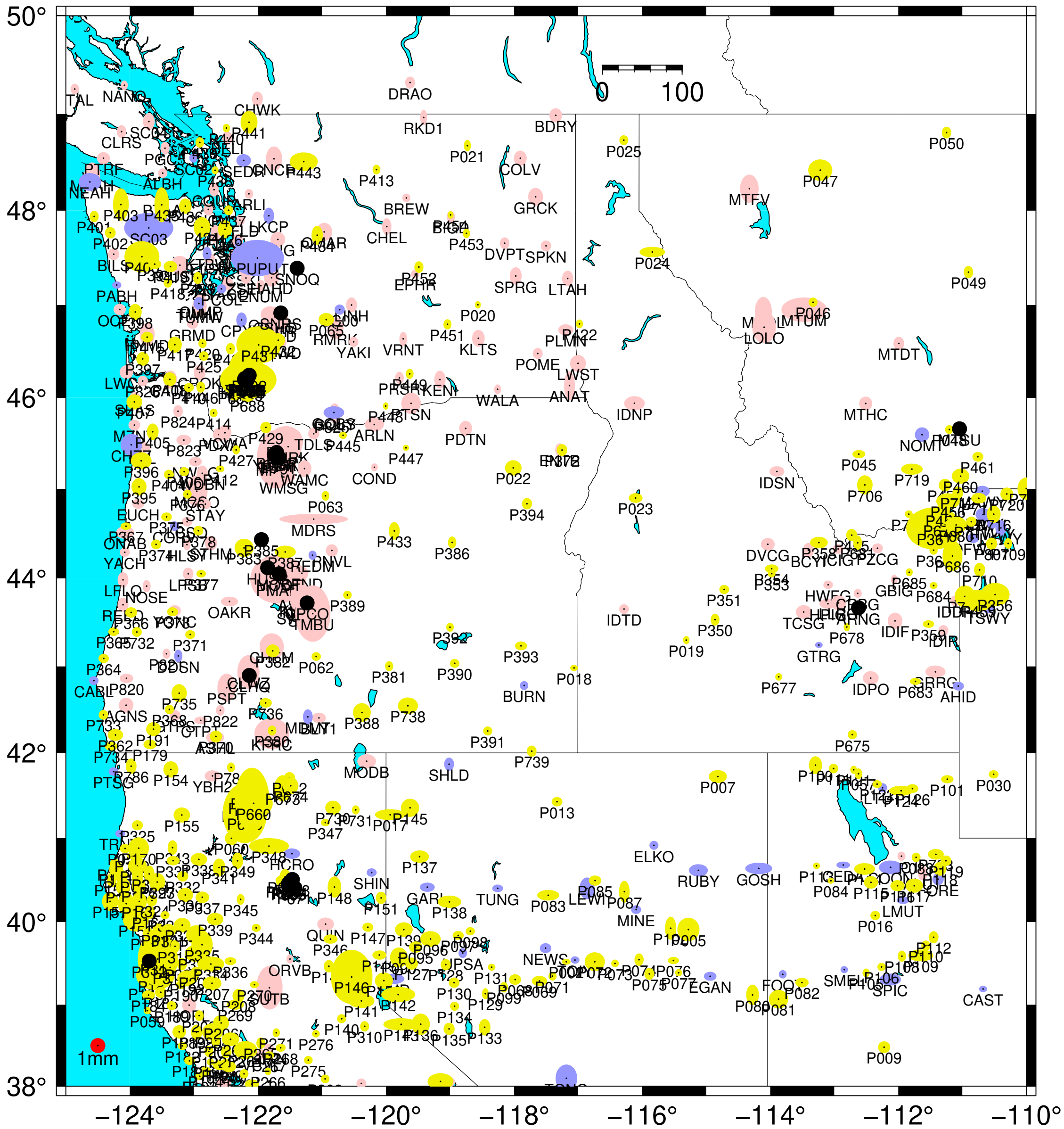

Figure 2: Distribution of the RMS scatters of horizontal position estimates from the CWU analysis for the Northern Western United States. The color of the ellipses that give the north and east RMS scatters denotes the network given by the legend in the figure. The small red circle shows the size of 1 mm scatters. Sites shown with black circles have combined RMS scatters in north and east greater than 5 mm or are sites that have no data during this 3-month interval.

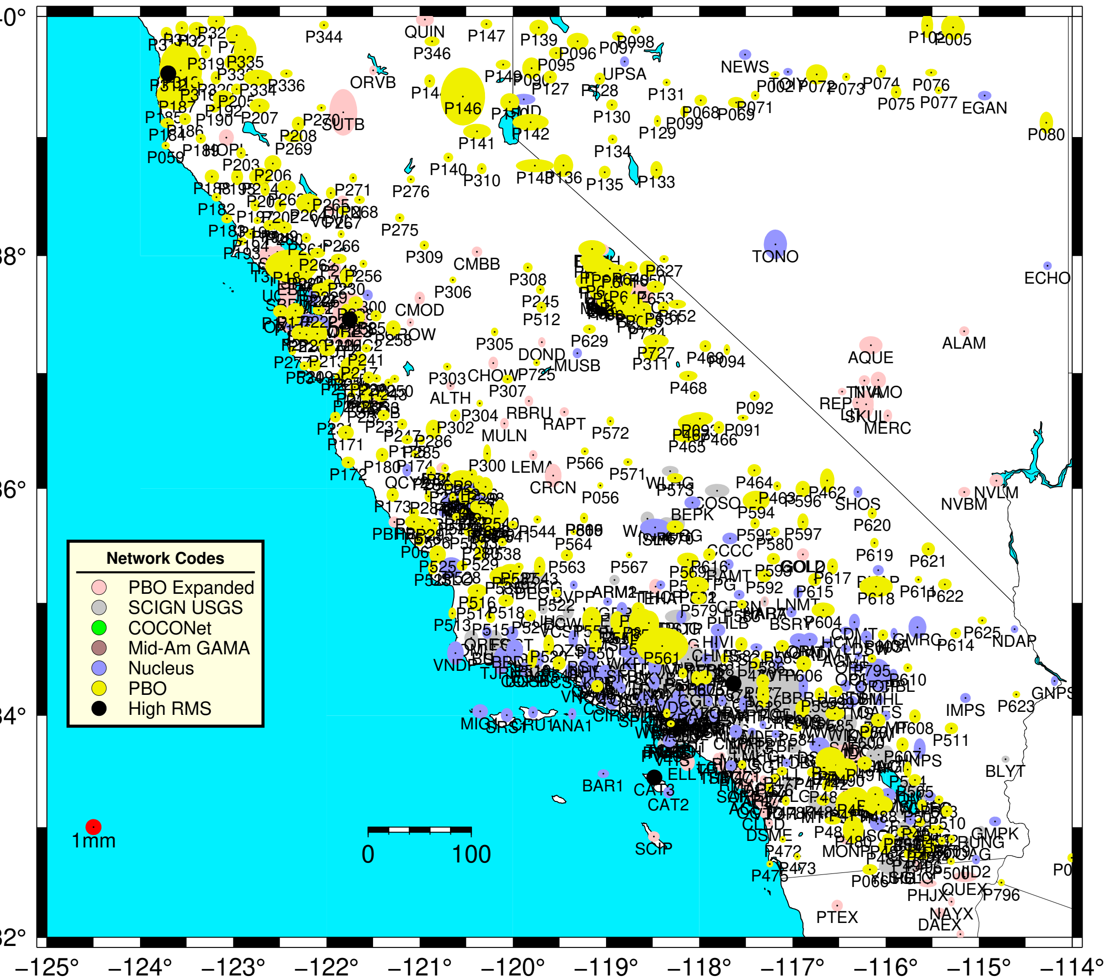

Figure 3: Same as Figure 4 except for the Southern Western United States. Black circles show large RMS scatter sites.

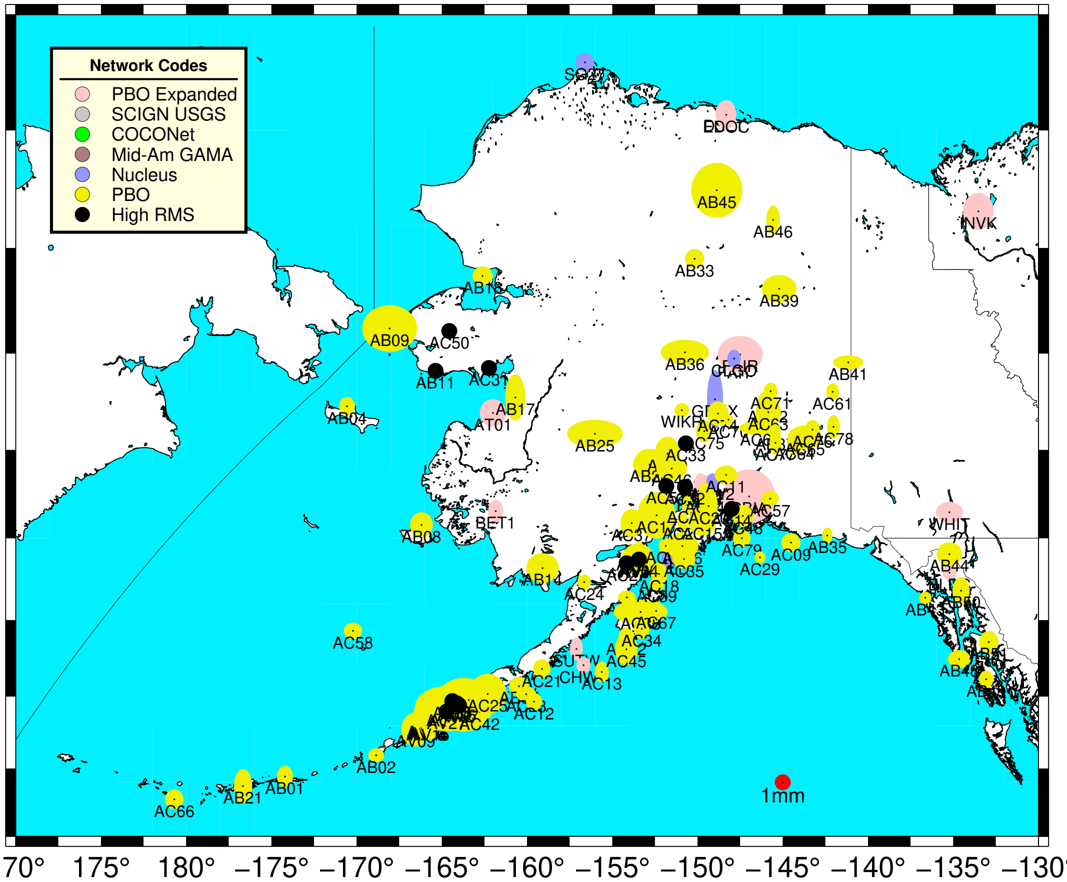

Figure 4: Same as Figure 4 except for the Alaskan region.

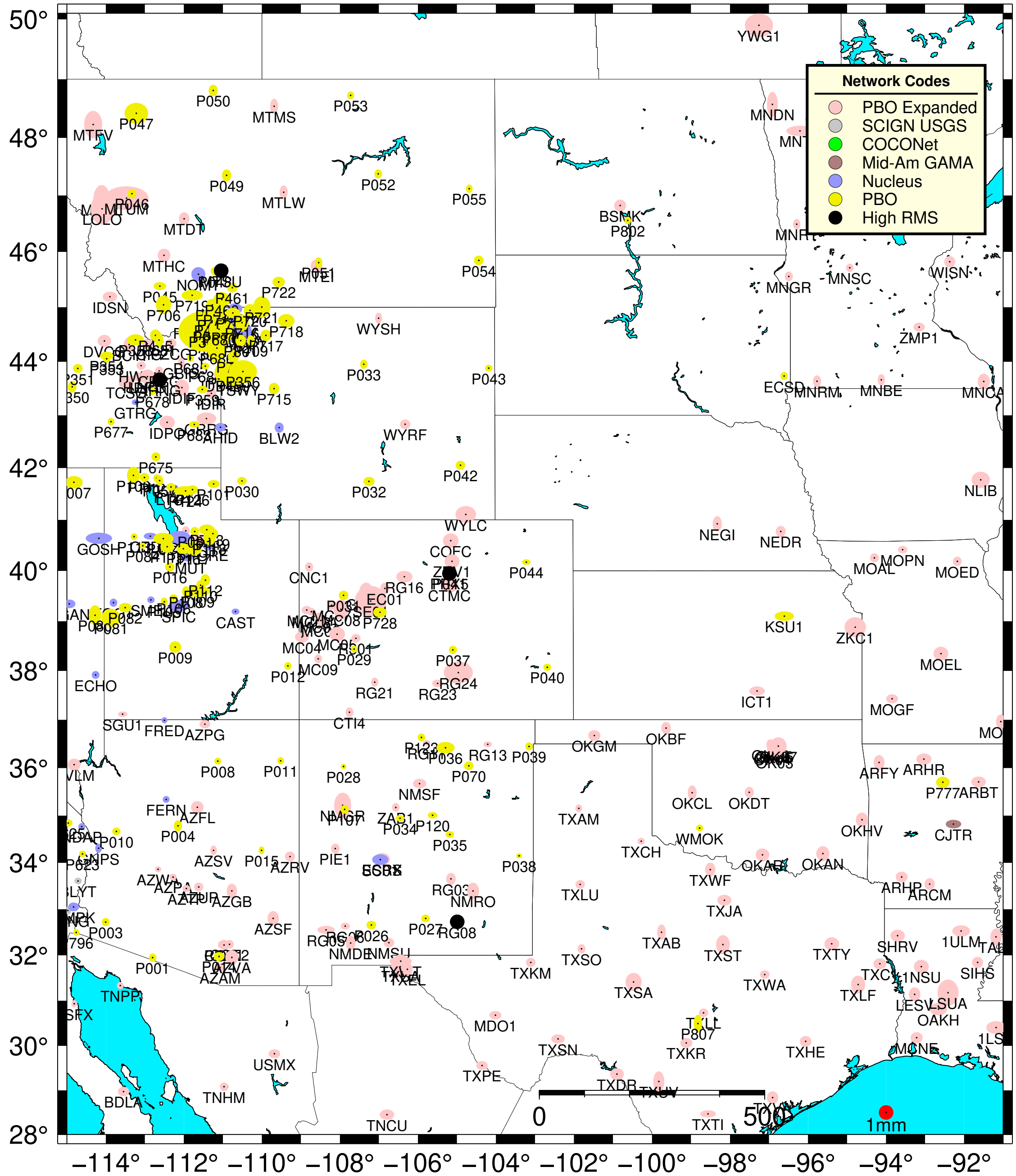

Figure 5: Same as Figure 4 except for the Central United States

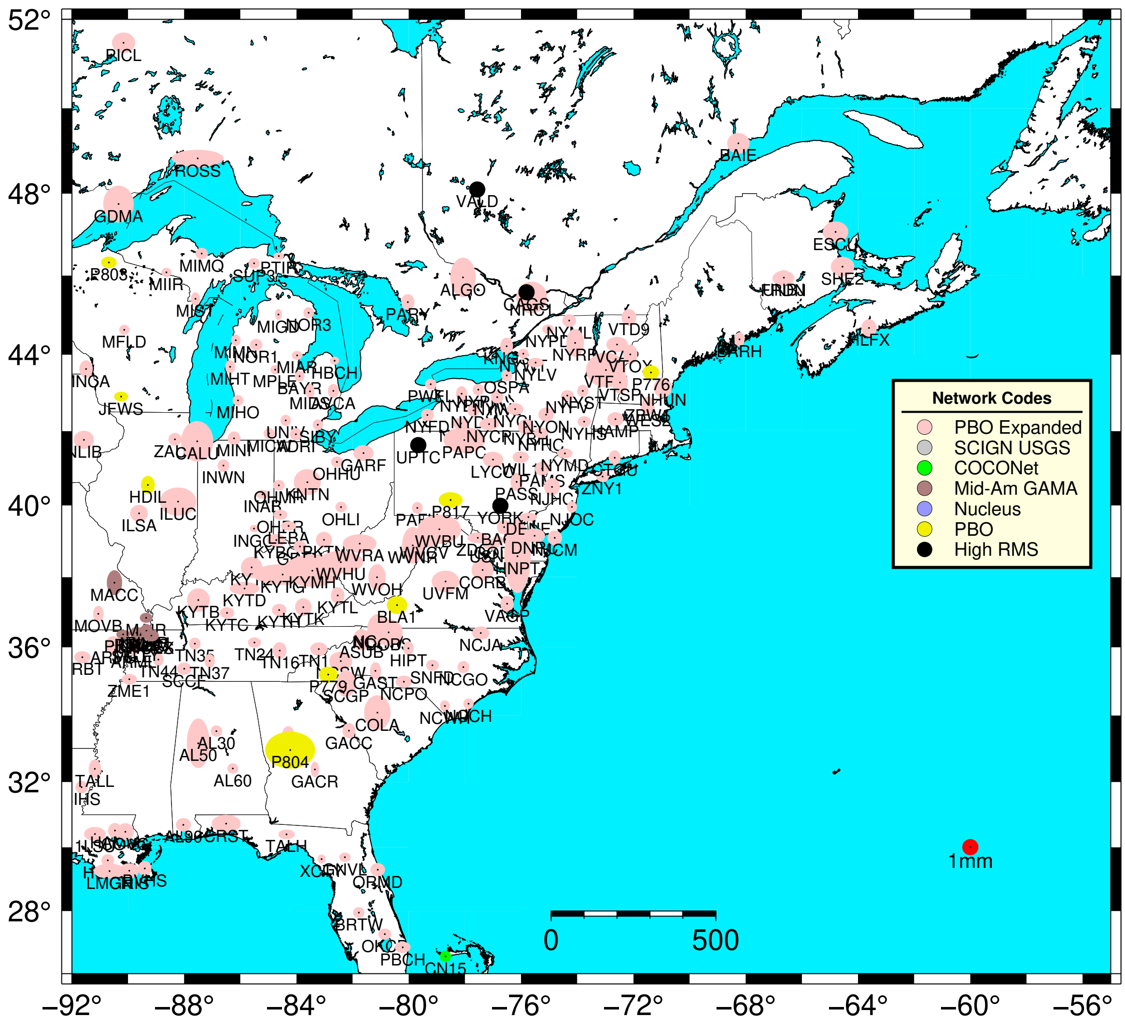

Figure 6: Same as Figure 4 except for the Eastern United States

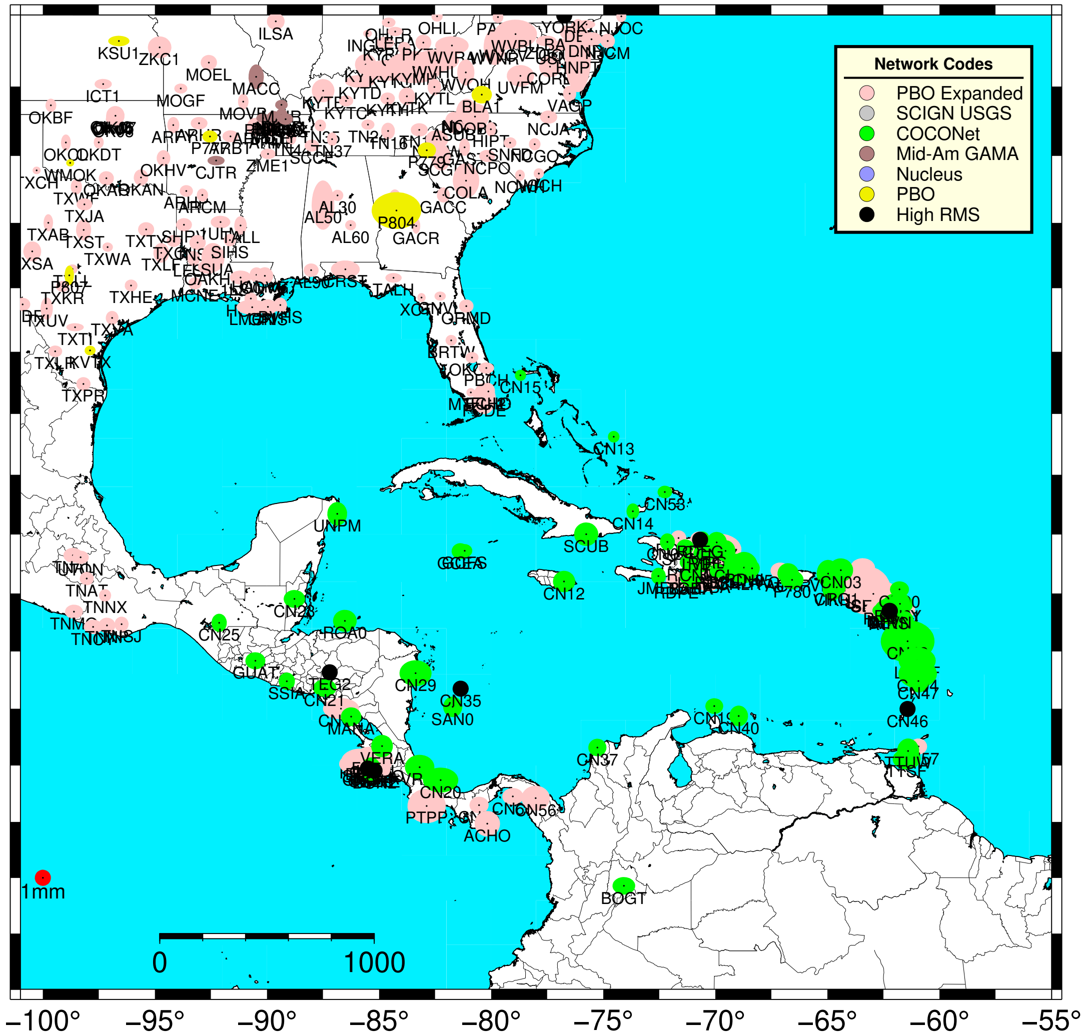

Figure 7: Same as Figure 4 except for the Caribbean region.

GLOBK Apriori coordinate file and earthquake files

As part of the quarterly analysis, we run a complete analysis of the time series files and generate position, velocity, and other parameter estimates from these time series. These files can be directly used in the GLOBK analysis files sent with the GAGE analysis documentation. The current earthquake and discontinuity files used in the GAGE ACC analyses are All_NOTA_eqs.eq All_NOTA_ants.eq All_NOTA_unkn.eq. These names have been changed to reflect that they now refer to the Network of America and no longer just the plate boundary observatory. The GLOBK apriori coordinate file All_CWU_nam14.apr is the current estimate based on data analysis in this quarterly report.

Snapshot velocity field analysis from the reprocessed PBO analysis.

For this quarterly report, we generate velocity estimates for the reprocessed results and the current GAGE analyses that are in the NAM14 reference frame using the CWU analysis. There are 2742 stations in the CWU solution. The statistics of the fits to results are shown in Table 3. Because these are cumulative statistics, they are little changed from last quarter. In this analysis, offsets are estimated for antenna changes and earthquakes. Annual signals are estimated, and for some earthquakes, logarithmic post-seismic signals are also estimated. The full tables of RMS fit, along with the duration of the data used, are given in cwu_nam14_241221.tab. The velocity estimates are shown by region and network type in Figures 8-14. The color scheme used is the same as Figures 2-7. The snapshot velocity field file for CWU is cwu_nam14_241221.snpvel.

Table 3: Statistics of the fits of 2742 stations analyzed CWU in the reprocessed analysis for data collected between Jan 1, 1996 and March 22, 2025.

Center	North (mm)	East (mm)	Up (mm)
Median (50%)			
CWU	1.42	1.39	6.28
70%			
CWU	1.80	1.76	7.17
95%			
CWU	4.23	3.85	11.82

In Figures 8-14, different tolerances are used for maximum standard deviation in each figure so that regions with small velocity vectors can be displayed at large scales without the plots being dominated by large error bar points. The standard deviations of the velocity estimated are computed using the GLOBK First-order-Gauss-Markov Extrapolation (FOGMEX) model that aims to account for temporal correlations in the time series residuals. This algorithm is also called the "Realistic Sigma" model.

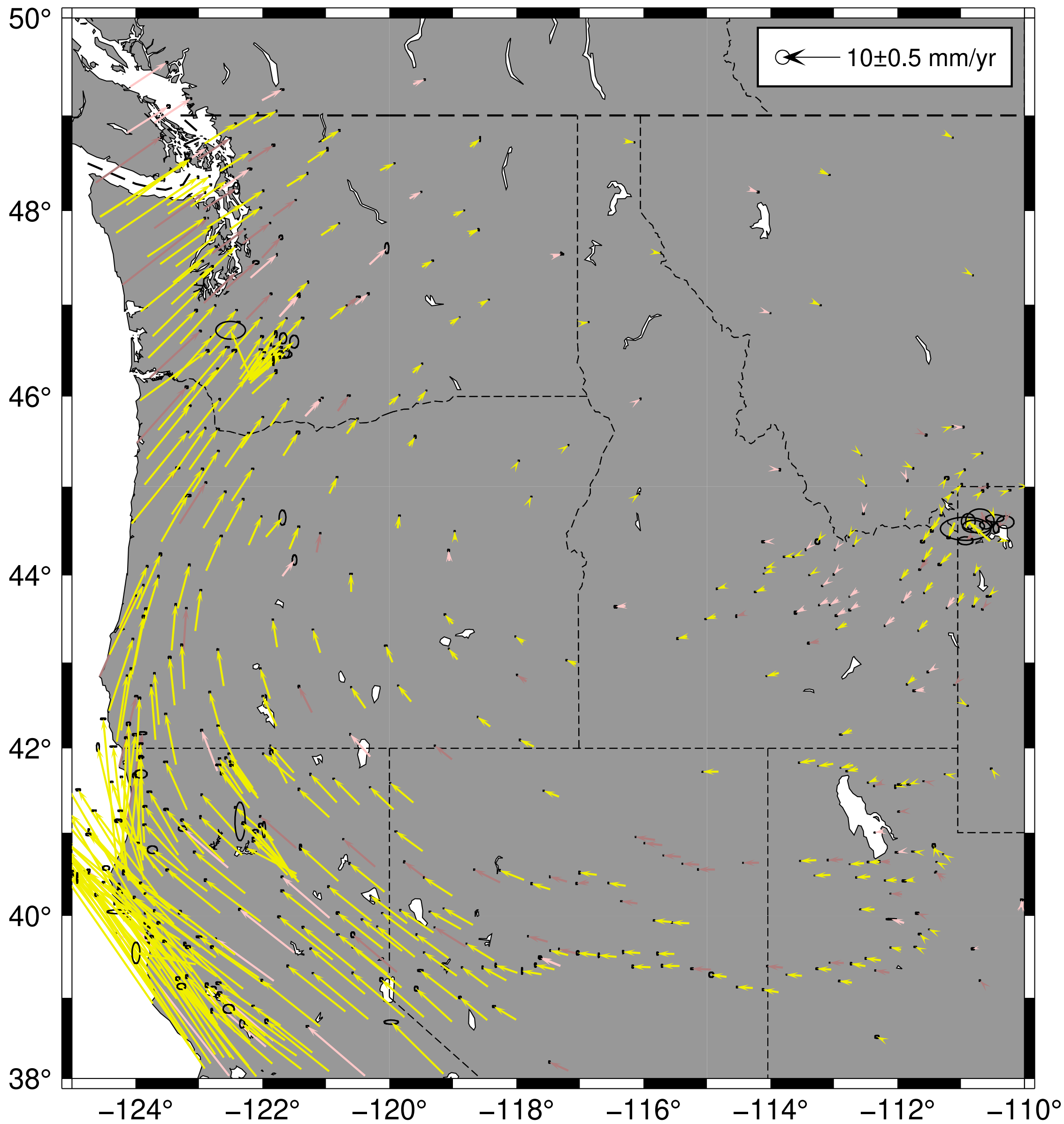

Figure 8: Velocity field estimates for the Pacific Northwest from the CWU solution generated using time series analysis and the FOGMEX error model. 95% confidence interval error ellipses are shown. The color scheme of the vectors matches the network type legend in Figure 4. Only velocities with horizontal standard deviations less than 2 mm/yr are shown (this value is reduced from previous reports due to the improved velocity sigmas).

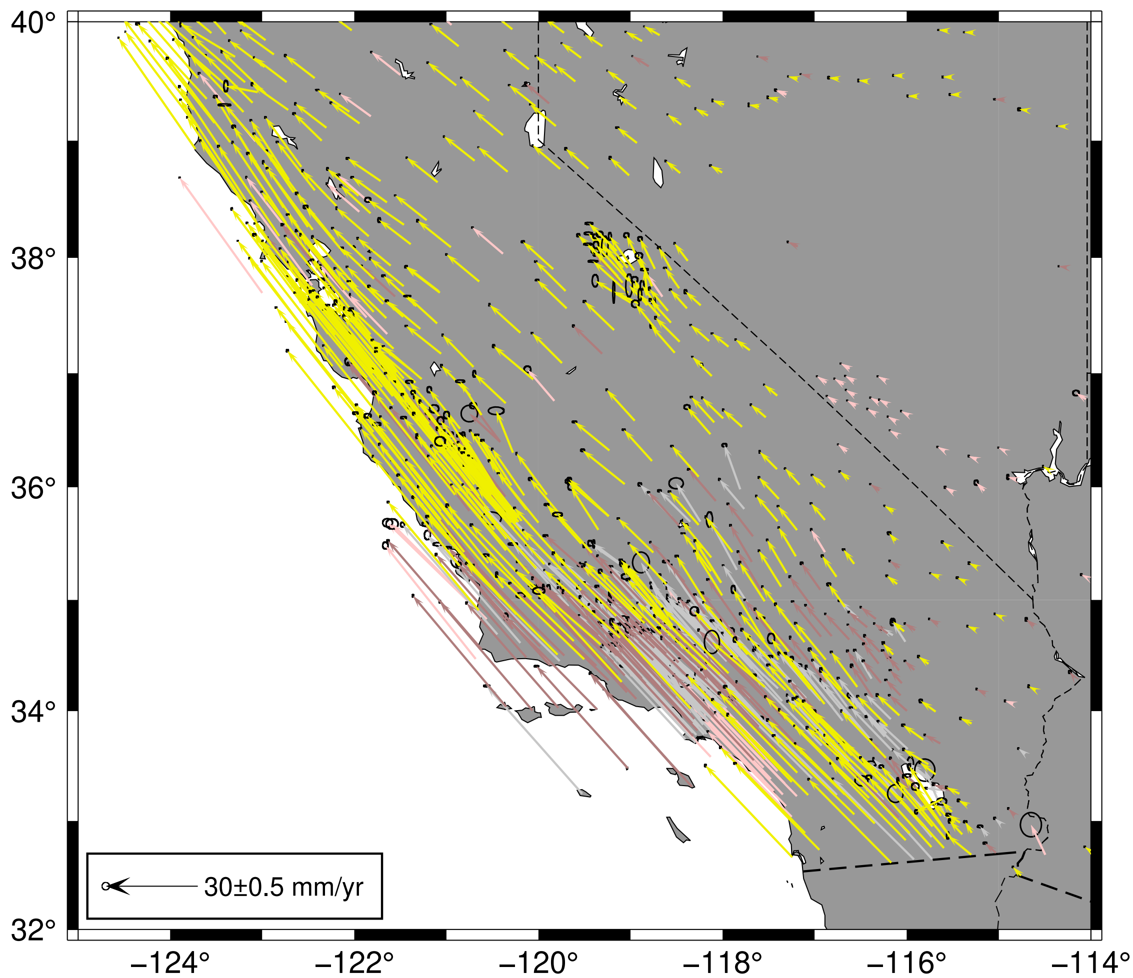

Figure 9: Same as Figure 8 except for South Western United States. Only velocities with horizontal standard deviations less than 2 mm/yr are shown.

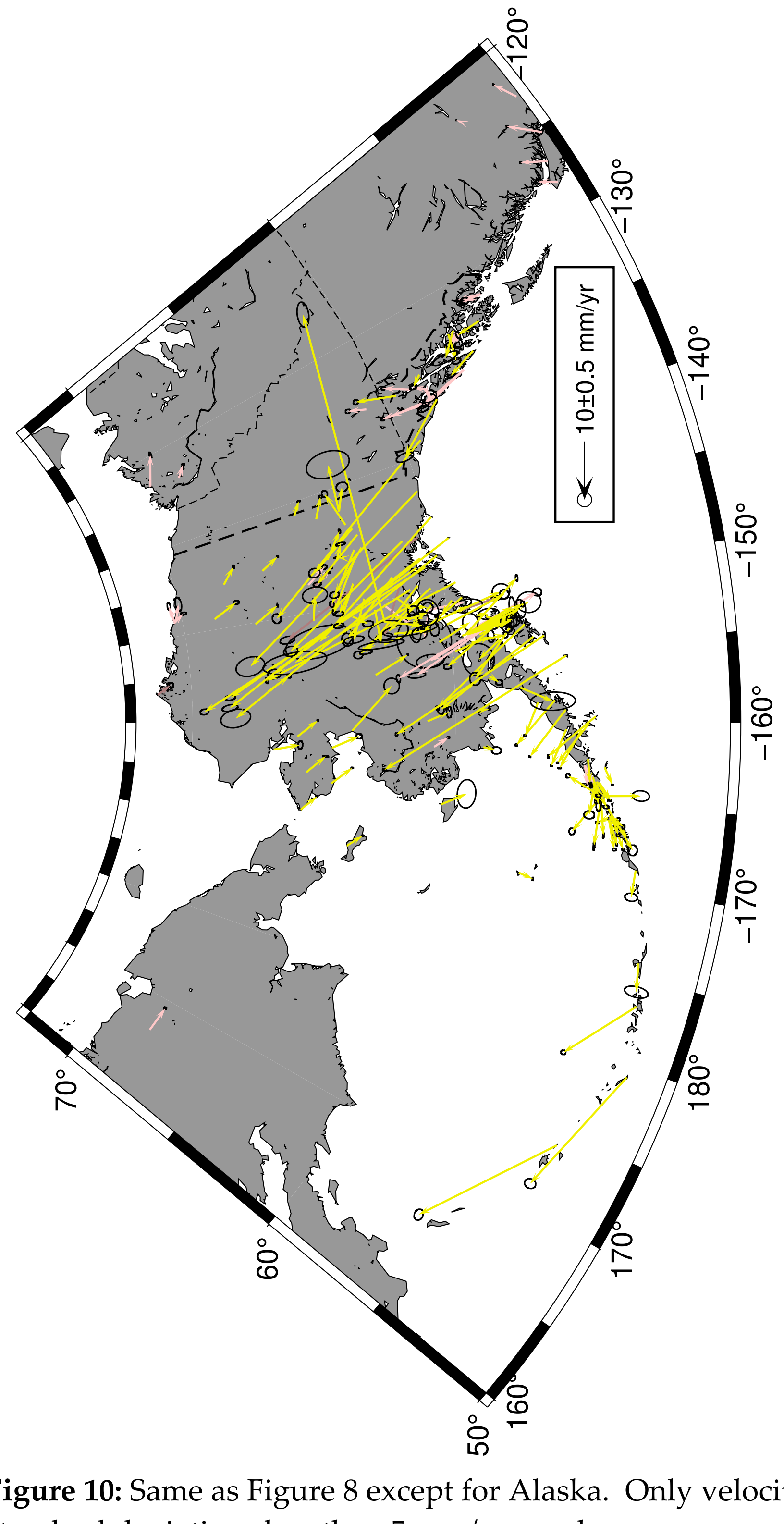

Figure 10: Same as Figure 8 except for Alaska. Only velocities with horizontal standard deviations less than 5 mm/yr are shown

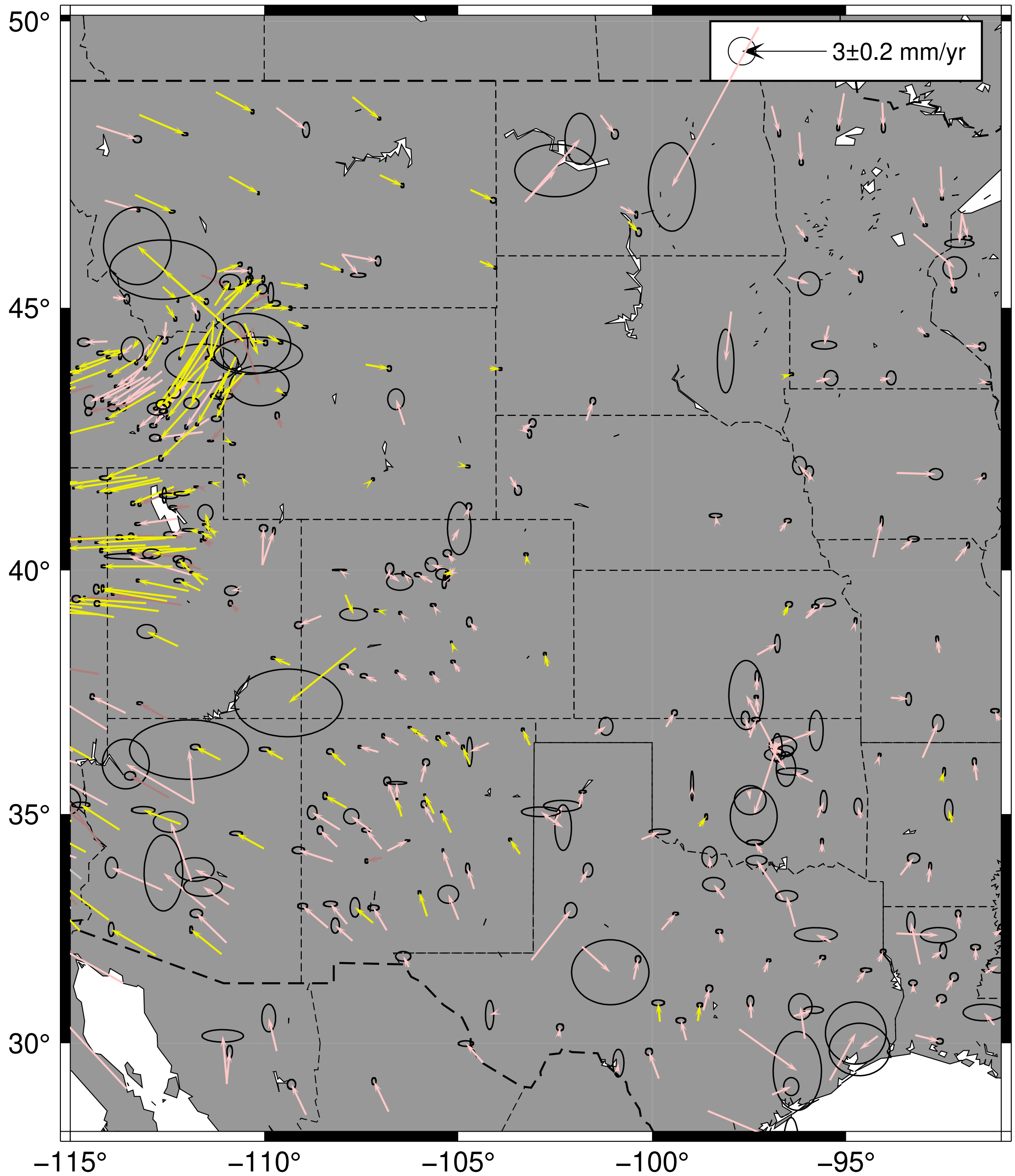

Figure 11: Same as Figure 8 except for Central United States. Only velocities with horizontal standard deviations less than 1 mm/yr are shown.

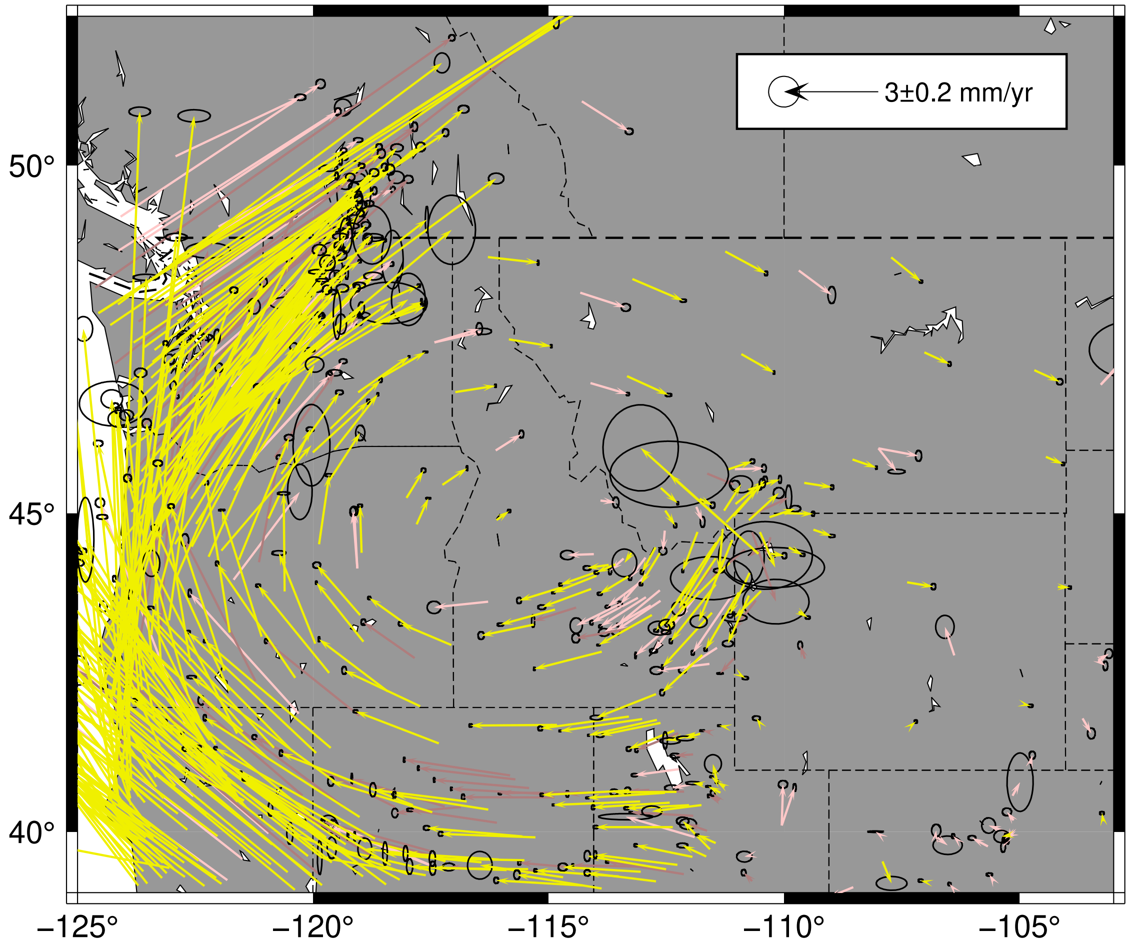

Figure 12: Same as Figure 8 except for Western Central United States. Only velocities with horizontal standard deviations less than 1 mm/yr are shown. Anomalous vectors at longitude 250º are in the Yellowstone National Park and most likely are showing volcanic processes.

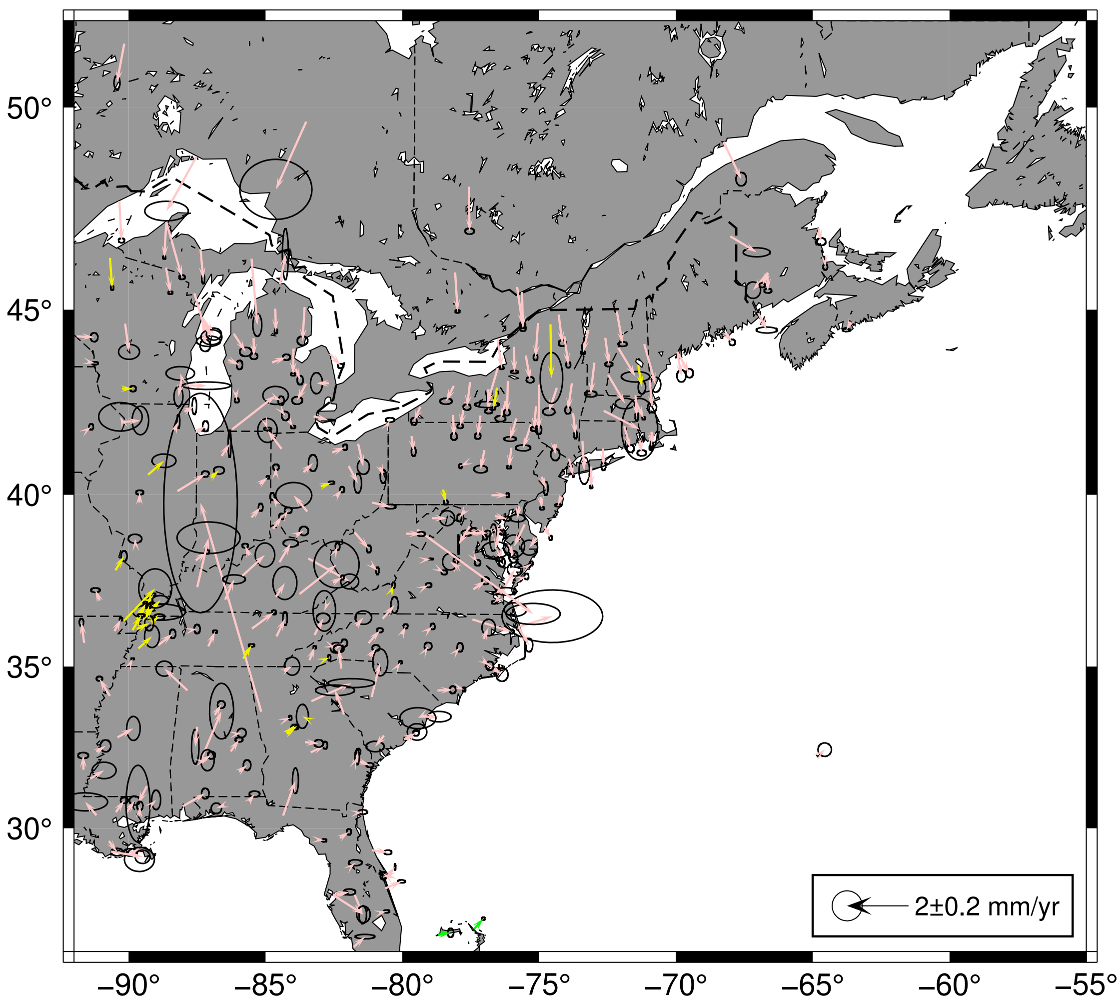

Figure 13: Same as Figure 8 except for the Eastern United States. Only velocities with horizontal standard deviations less than 2 mm/yr are shown. The systematic velocity of sites in the Northeast and central US show deviations for current GIA models in the horizontal velocities.

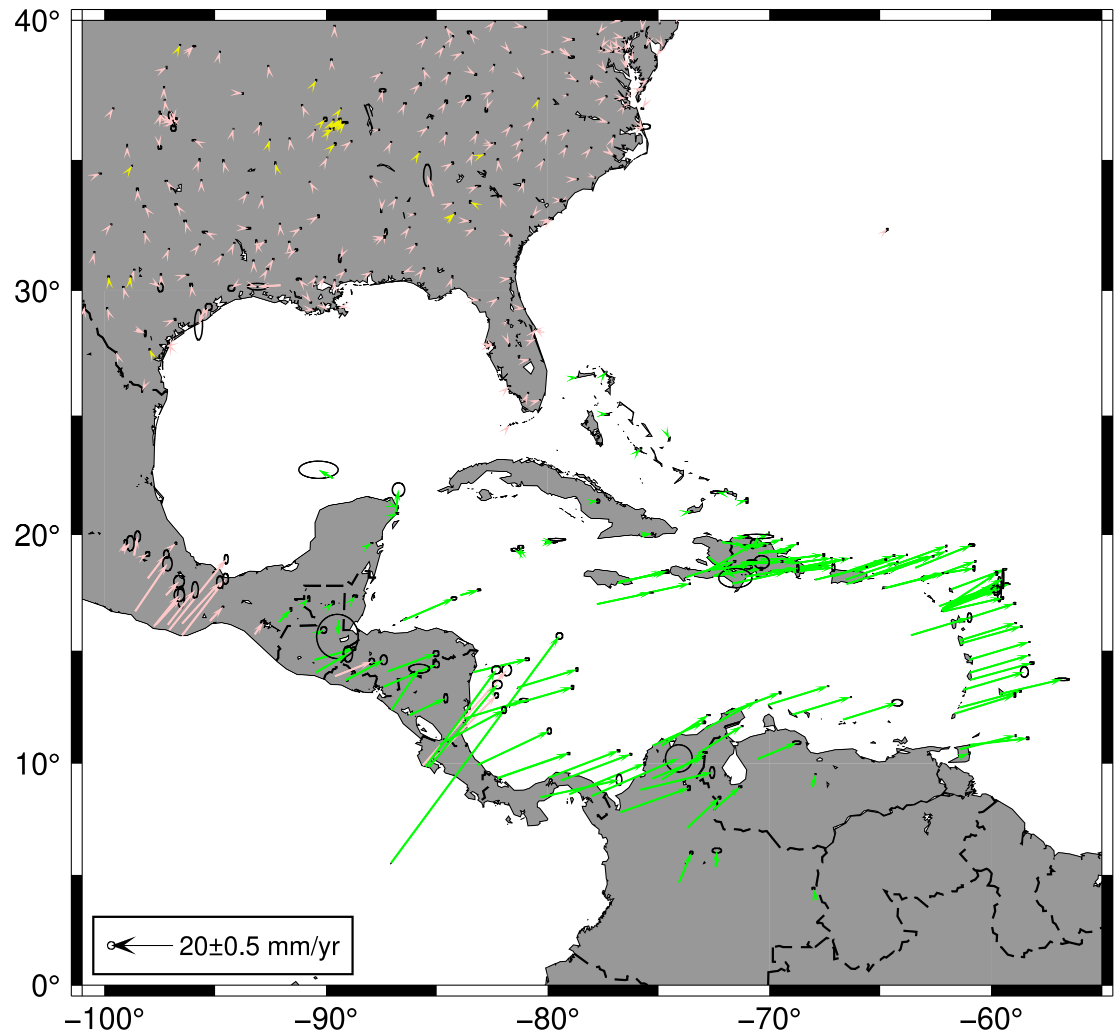

Figure 14: Same as Figure 8 except for the Caribbean region. Only velocities with horizontal standard deviations less than 5 mm/yr are shown.

Earthquake Analyses: 2024/09/15-2025/03/15

We use the NEIC catalog to search for earthquakes that could cause coseismic offsets at the sites analyzed by the GAGE analysis centers. Of the 26 earthquakes examined during this quarter, one generated co-seismic offsets greater than 1 mm. The earthquake EQ76 ANSS(ComCat) us7000pcdl mww7.6 209 km SSW of George Town, Cayman Islands; date and time 2025/02/08 23:24 displaced 5 stations with two having displacements greater than 10 mm. The largest displacement was 21 mm at station GCEA.

Antenna and other discontinuity events.

Antenna swaps at 10 sites have been added to the list of offsets estimated when fitting velocities and other parameters to the CWU time series. These offsets were spread throughout the quarter. An additional 38 breaks were added to the All_NOTA_unkn.eq file.

Anomalous sites

The following sites have been noted as having anomalous motions during this quarter. We updated the ACC_GAGE website to show times of earthquakes, antenna changes, and offsets for unknown reasons. Plots for CWU are now generated with and without offsets (computed from the Kalman filter time series analysis) removed. The landing page for http://geoweb.mit.edu/~tah/ACC_GAGE/ now has the following explanation.

Analyses from Central Washington University (CWU). Series are:
NMT -- Old plots from New Mexico Tech Analyses (Ends 9/15/2018).
PBO -- Old plots from Combined NMT+CWU analyses (Ends 9/15/2108).
CWURAW -- Raw time series with linear trend removed
CWUOFF -- Time series with linear trend and offsets from cwu.kalts_nam14.off removed
Vertical lines denote times of offsets in time series:
Purple, solid: Earthquakes (OffEq ! EQ)
Blue, dotted: Antenna changes (Break ! AN)
Cyan, dashed: Breaks for unkown reasons (Break ! UN)

N after site name means NOTA operated site, U means UNAVCO/Earthscope log file.

Site	**N**	**Issues related to site**
		2025-01-17
OBSR	U	Mt. Rainier site with 'box car' east seasonal. https://geoweb.mit.edu/~tah/ACC_GAGE/OBSR.CWUOFF.png
WWFG	U	Salton Sea site; large gap and jump a month after antenna replacement. https://geoweb.mit.edu/~tah/ACC_GAGE/WWFG.CWUOFF.png
		2025-01-24
CAND	U	LAND, HUNT and CARH Added unknown breaks 2024-10-13 for apparent antenna change that is not in logs. For HUNT, TBLP, and CARH "undoes" unknown offset from 2023-08-12. There are no recent UNR results; JPL shows jump 4 days before CWU. https://geoweb.mit.edu/~tah/ACC_GAGE/CAND.CWUOFF.png https://geoweb.mit.edu/~tah/ACC_GAGE/HUNT.CWURAW.png

		
SKUL	U	Site was noisy after gap, but then improved and is now noisy again (although not as bad when looked at closely). https://geoweb.mit.edu/~tah/ACC_GAGE/SKUL.CWUOFF.png
		2025-01-31
ROSS		Site on great lakes maybe showing water level changes? CORS site. https://geoweb.mit.edu/~tah/ACC_GAGE/ROSS.CWUOFF.png
		2025-02-07
CUHS	U	Very strong systematic annual and longer period signals. VCST 20 km away seems to be in a similar environment but does not large systematics. https://geoweb.mit.edu/~tah/ACC_GAGE/CUHS.CWUOFF.png
P488	N	Jump in east with no meta data change. Add UNKN break. Site west of Salton sea. P487 (10km away) does not have jump. https://geoweb.mit.edu/~tah/ACC_GAGE/P488.CWUOFF.png
		2025-02-14
GCEA		Earthquake offset: added to list EQ76 ANSS(ComCat) us7000pcdl mww7.6 209 km SSW of George Town, Cayman Islands; date and time 2025/02/08 23:24. Rapid coseismic solution sent. GCFS also offset; each by about 15 mm. https://geoweb.mit.edu/~tah/ACC_GAGE/GCEA.CWUOFF.png https://geoweb.mit.edu/~tah/ACC_GAGE/GCFS.CWUOFF.png
		2025-02-24 Not in telecon
AB01		Site in Atka Islands in the Aleutians. Restarted and probably OK due to volcanic activity. https://geoweb.mit.edu/~tah/ACC_GAGE/AB01.CWUOFF.png
AB45	N	Northern Alaska, outliers in East. Could be snow/ice. https://geoweb.mit.edu/~tah/ACC_GAGE/AB45.CWUOFF.png
P142	N	Very skewed in East.

		https://geoweb.mit.edu/~tah/ACC_GAGE/P142.CWUOFF.png
RKMG		Very non-steady motion. Site in southern part of LA basin. https://geoweb.mit.edu/~tah/ACC_GAGE/RKMG.CWUOFF.png
WNRA		Site near Whittier Narrows. Systematic residuals but with 30 mm east offset in last rapid https://geoweb.mit.edu/~tah/ACC_GAGE/WNRA.CWUOFF.png
		2025-02-28 (none) 2025-03-07 (no new) (AT01 and P219 reported before)
		2025-03-14
AC33	N	Site in Denali National park. Snow recently but looks like monument may have been bent in 2018 and 2019 snow season. http://geoweb.mit.edu/~tah/ACC_GAGE/AC33.CWUOFF.png
AC51	N	Similar region to AC33. Long term systematics with “rate changes”. http://geoweb.mit.edu/~tah/ACC_GAGE/AC51.CWUOFF.png
CPCO	U	Site south of Bend, OR. Starting to behave erratically. Nearby sites don’t show this behavior. http://geoweb.mit.edu/~tah/ACC_GAGE/CPCO.CWUOFF.png
GCEA		Site in Caribbean. Offset due to EQ76 (us7000pcdl mww7.6 209 km SSW of George Town, Cayman Islands). GCEF also offset. http://geoweb.mit.edu/~tah/ACC_GAGE/GCEA.CWUOFF.png
P479	N	Maybe North offset on 2024 03 23 (only site). No metadata changes. http://geoweb.mit.edu/~tah/ACC_GAGE/P479.CWUOFF.png
P488	N	New jump at 2025 53 (02/22) but there is antenna changes 2025 63 (03/04). Could date of change be wrong. http://geoweb.mit.edu/~tah/ACC_GAGE/P488.CWUOFF.png
RG08	N	Continued bad antenna. http://geoweb.mit.edu/~tah/ACC_GAGE/RG08.CWUOFF.png
WNRA	U	LA Whitter narrows site. 100-160 mm offsets in North and East (in two stages in East). Nothing at RHCL. Jumps om 2025 02 21 and 2025 03 11. http://geoweb.mit.edu/~tah/ACC_GAGE/WNRA.CWUOFF.png
		2025-03-21 Not in telecon (no new; just snow)
		2025-03-28
TWIW		On flank of Mt. St. Helens. Structure is probably real deformation. P695, P696 and P692 share common height signal and other shorter period variations. https://geoweb.mit.edu/~tah/ACC_GAGE/TWIW.CWUOFF.png
		2025-04-04
LUTZ		South of San Francisco. Large and growing offsets in east and north. NCEDC site. P226 5 km away shows no anomaly. https://geoweb.mit.edu/~tah/ACC_GAGE/LUTZ.CWUOFF.png
WIKR	U	Site near Denali Fault Alaska. Most likely snow recently but site has long term east curvature. https://geoweb.mit.edu/~tah/ACC_GAGE/WIKR.CWUOFF.png

GNSS Rapid processing

Since 2021/10/20, CWU has generated a combined GPS and Galileo rapid solution because JPL has made available orbit and clock files from a global GPS and Galileo solution. These solutions are experimental, and for a number of sites, there are systematic mean differences in position between the GPS-only and the combined solutions. For this reason, these combined solutions are not distributed through the EarthScope GAGE products portal. Initially, there were inconsistencies in the GPS-only and combined analyses (e.g., elevation angle cutoff) that affected the comparison of the results, specifically when comparing mean positions and WRMS scatters of the fits to linear trends. Starting on 2024/03/26, these inconsistencies were resolved and since that time, a direct comparison of the GPS-only and combined GPS and Galileo solutions is possible. Results of the comparisons are reported daily to the GAGE_ACS email list. With nine months of consistently processed results available, we compare the results below. The current analysis used 867 stations with up to 275 days of comparison. The median NEU scatters for the GPS+GAL solutions are 0.89, 0.89, and 4.94 mm. The corresponding values from the common GPS-only solutions are 0.97, 0.95, and 5.21 mm, slightly larger than those from the GPS+GAL solution.

Table 4: Mean differences between GPS-only and GPS+Galileo rapid solutions. Differences are taken as GPS+GAL minus GPS-only position estimates. The largest 10 positive and negative differences in Up, North, and East are shown. The sig column is the standard deviation of the mean (assuming white noise statistics), wrms is the weighted root-mean-square scatter about the mean, and nrms is the normalized root mean square ($\sqrt{\chi^2/f}$).

CWU GNSSR Analysis Tue Apr 8 22:25:35 EDT 2025

Stat	enu	#	MeanDiff (mm)	sig (mm)	wrms (mm)	nrms	Receiver	Antenna	Radome
Stat	enu	#	MeanDiff (mm)	sig (mm)	wrms (mm)	nrms	Receiver	Antenna	Radome
FLIN	U	362	-13.56	0.13	2.45	0.2	SEPT POLARX5	NOV750.R4	NOVS
SASK	U	362	-12.88	0.12	2.19	0.2	JAVAD TRE_G3TH DELTA	NOV750.R4	NOVS
ARBT	U	281	-9.42	0.28	4.76	0.5	TRIMBLE NETR9	TRM115000.00	NONE
1LSU	U	228	-7.57	0.41	6.15	0.5	TRIMBLE ALLOY	TRM115000.00	NONE
HDIL	U	100	-7.53	0.63	6.33	0.5	SEPT POLARX5	TRM59800.80	SCIT
PTRF	U	300	-7.12	0.26	4.44	0.4	SEPT POLARX5S	SEPCHOKE_B3E6	SPKE
MHMS	U	360	-6.42	0.17	3.16	0.3	SEPT POLARX5	TWIVC6050	SCIT
VDCY	U	362	-6.23	0.21	4.05	0.3	SEPT POLARX5	TRM59800.99	SCIT
CN29	U	236	-6.01	0.65	10.06	0.7	TRIMBLE NETR9	TRM59800.99	SCIT
SAB1	U	269	-5.61	0.36	5.84	0.5	SEPT POLARX5S	SEPCHOKE_B3E6	SPKE
....									
ARML	U	341	5.91	0.21	3.87	0.4	SEPT POLARX5	SEPPOLANT_X_MF	NONE
P224	U	360	6.00	0.22	4.18	0.4	TRIMBLE NETR9	TRM59800.00	SCIT
LCHS	U	327	6.11	0.24	4.39	0.5	SEPT POLARX5	SEPPOLANT_X_MF	NONE
NWCC	U	19	6.14	0.49	2.12	0.2	SEPT POLARX5	SEPPOLANT_X_MF	NONE
HCES	U	73	6.47	0.45	3.86	0.4	SEPT POLARX5	SEPPOLANT_X_MF	NONE
CHZZ	U	359	6.53	0.40	7.49	0.5	TRIMBLE NETR9	TRM59800.80	SCIT
MCTY	U	324	8.24	0.27	4.91	0.5	SEPT POLARX5	SEPPOLANT_X_MF	NONE
P385	U	362	8.36	0.50	9.42	1.0	SEPT POLARX5	TRM59800.80	SCIT
P312	U	358	12.75	1.94	36.67	1.1	TRIMBLE NETR9	TRM59800.80	SCIT
COLA	U	361	14.60	0.67	12.72	1.4	TRIMBLE ALLOY	TRM55971.00	NONE

Stat	enu	#	MeanDiff	sig	wrms	nrms	Receiver	Antenna	Radome

			(mm)	(mm)	(mm)				
LONG	N	359	-2.70	0.18	3.41	1.1	SEPT POLARX5	TWIVC6050	SCPL
COLA	N	361	-2.18	0.08	1.57	0.7	TRIMBLE ALLOY	TRM55971.00	NONE
P033	N	361	-1.61	0.10	1.93	0.8	TRIMBLE NETR9	TRM59800.80	SCIT
P669	N	362	-1.57	0.04	0.80	0.3	SEPT POLARX5	TWIVC6050	SCIS
AB48	N	5	-1.56	1.43	1.20	0.3	SEPT POLARX5	TRM29659.00	SCIT
P312	N	358	-1.56	0.30	5.72	0.9	TRIMBLE NETR9	TRM59800.80	SCIT
AB18	N	282	-1.50	0.05	0.79	0.2	SEPT POLARX5	TRM59800.99	SCIT
SELD	N	307	-1.45	0.06	1.04	0.3	SEPT POLARX5	TRM159800.00	SCIT
P224	N	360	-1.39	0.05	0.88	0.3	TRIMBLE NETR9	TRM59800.00	SCIT
AC34	N	254	-1.38	0.05	0.80	0.2	SEPT POLARX5	TRM29659.00	SCIT
....									
GOLD	N	356	1.27	0.02	0.44	0.2	JAVAD TRE_G3TH DELTA	AOAD/M_T	NONE
KYMH	N	259	1.29	0.07	1.18	0.5	TRIMBLE NETR9	TRM57971.00	NONE
GODE	N	347	1.32	0.03	0.62	0.2	SEPT POLARX5TR	AOAD/M_T	JPLA
P794	N	278	1.32	0.04	0.60	0.2	SEPT POLARX5	TRM59800.00	SCIT
P215	N	320	1.54	0.06	1.01	0.4	SEPT POLARX5	TRM59800.80	SCIT
OSPA	N	281	1.75	0.08	1.35	0.5	SEPT POLARX5	TWIVC6150	SCIS
P156	N	275	1.85	0.18	2.90	0.8	SEPT POLARX5	TRM59800.80	SCIT
P252	N	53	2.28	0.20	1.49	0.6	TRIMBLE NETR9	TRM29659.00	SCIT
NNVN	N	301	2.55	0.26	4.55	1.6	ALERTGEO RESOLUTE	LEIAR20	LEIM
P385	N	362	2.73	0.14	2.60	1.0	SEPT POLARX5	TRM59800.80	SCIT

Stat	enu	#	MeanDiff (mm)	sig (mm)	wrms (mm)	nrms	Receiver	Antenna	Radome
CAT3	E	361	-2.45	0.43	8.12	1.0	TRIMBLE ALLOY	TRM59800.80	SCIT
P669	E	362	-1.84	0.05	0.90	0.3	SEPT POLARX5	TWIVC6050	SCIS
P187	E	361	-1.53	0.15	2.81	0.9	SEPT POLARX5	TRM59800.99	SCIT
KVTX	E	362	-1.49	0.03	0.66	0.3	SEPT POLARX5	TRM59800.99	SCIT
RDF2	E	74	-1.42	0.18	1.51	0.5	TRIMBLE NETR9	TRM57971.00	NONE
TFNO	E	210	-1.37	0.05	0.70	0.3	SEPT POLARX5	SEPCHOKE_B3E6	SPKE
AB48	E	5	-1.24	0.90	0.68	0.3	SEPT POLARX5	TRM29659.00	SCIT
P011	E	360	-1.24	0.04	0.69	0.3	SEPT POLARX5	TRM59800.80	SCIT
RG08	E	362	-1.23	0.11	2.18	1.0	SEPT POLARX5	TRM59800.99	SCIT
P051	E	360	-1.22	0.02	0.44	0.2	SEPT POLARX5	TRM59800.00	SCIT
....									
KOKB	E	239	1.15	0.07	1.09	0.5	SEPT POLARX5TR	ASH701945G_M	NONE
P740	E	349	1.17	0.07	1.36	0.5	SEPT POLARX5	TRM59800.99	SCIT
P071	E	360	1.18	0.02	0.34	0.1	SEPT POLARX5	TRM59800.99	SCIT
SPT0	E	361	1.19	0.04	0.72	0.4	SEPT POLARX5TR	TRM59800.00	OSOD
KIR0	E	361	1.20	0.04	0.72	0.4	SEPT POLARX5	JAVRINGANT_DM	OSOD
VIS0	E	360	1.33	0.04	0.78	0.4	SEPT POLARX5	JAVRINGANT_DM	OSOD
ONSA	E	360	1.40	0.04	0.77	0.4	SEPT POLARX5TR	AOAD/M_B	OSOD
NDAP	E	361	1.66	0.15	2.92	1.5	TRIMBLE NETR9	TRM59800.80	SCIT
EGAN	E	361	1.69	0.17	3.19	1.7	TRIMBLE NETR9	TRM59800.80	SCIS
P191	E	362	2.83	0.23	4.32	2.4	TRIMBLE NETR9	TRM59800.80	SCIT

ANET Processing

The ANET additional sites are being processed as a separate network, and the frame-resolved SINEX files will be given in the Antarctica 1984 reference frame (Altamimi *et al.*, 2016, 2017). We label this frame ant14. Time series and SINEX files are generated only for final orbit solutions and are labeled as fanet (instead of final to avoid name conflicts with loose solutions). The IGS14 loose submission files are labeled with "lse14" to differentiate them for the IGS08 loose submissions, which were labeled as loose. The statistics of the time series fits from the CWU solution for this quarter are given in Table 5.

Table 5: Statistics of the fits of 39 stations in the ANET region for CWU analyzed in the final orbit analysis between December 15, 2024 and March 22, 2025.

CWU	North (mm)	East (mm)	Up (mm)
Median ANET	1.24	1.19	6.11
70% ANET	1.36	1.37	6.57
95% ANET	2.31	2.62	8.28

The histograms of the RMS scatter in NEU of the results for this quarter are shown in Figure A.1

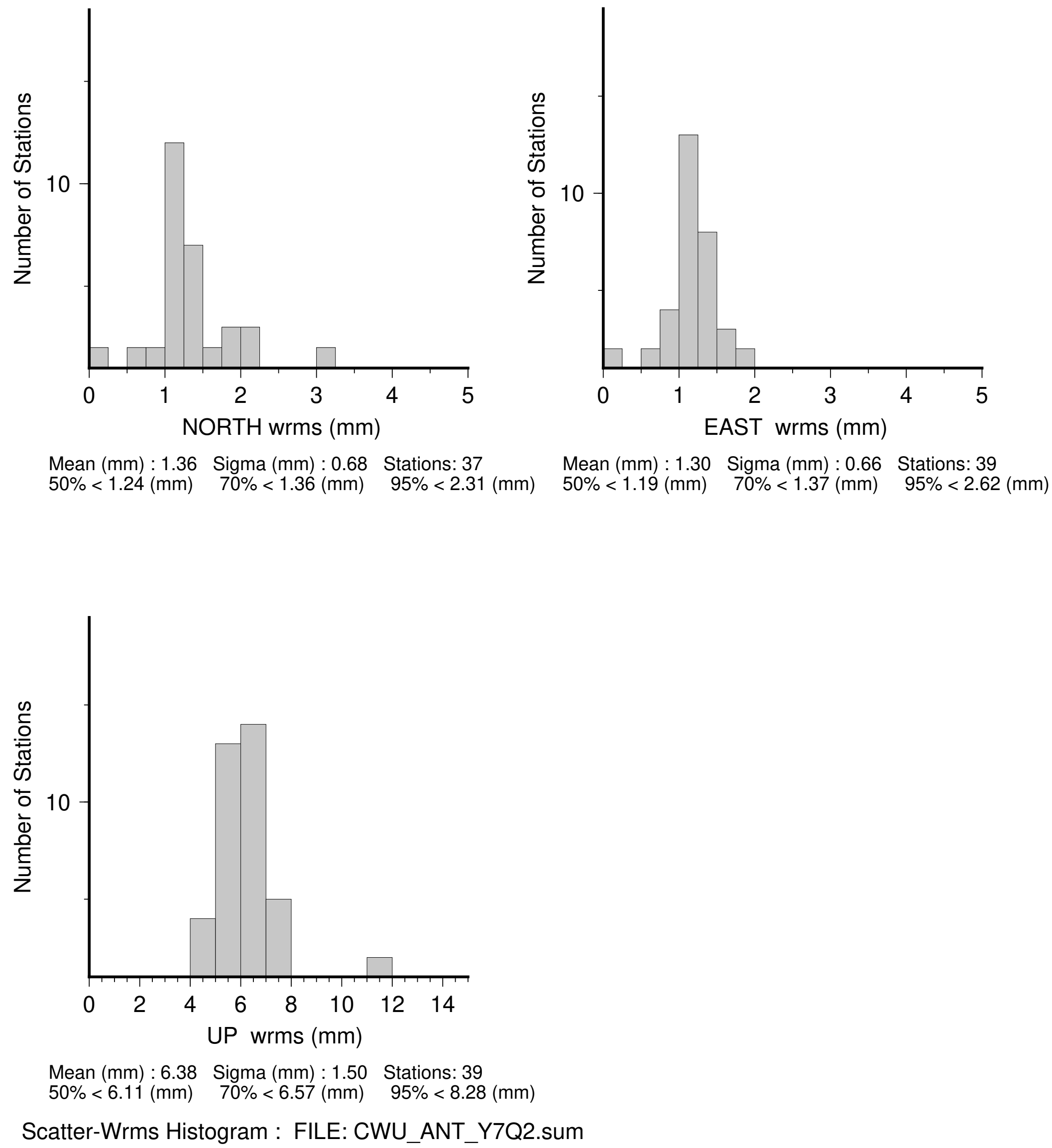

Figure A.1: CWU solution histograms of the North, East and Up RMS scatters of the position residuals for 39 stations in Antarctica analyzed between December 15, 2024 and March 22, 2025. Linear trends and annual signals were estimated from the time series.

References

Altamimi, Z., P. Rebischung, L. Metivier, and X. Collilieux (2016), ITRF2014: A new release of the International Terrestrial Reference Frame modeling nonlinear station motions, *J. Geophys. Res. Solid Earth*, 121, 6109-6131, doi: 10.1002/2016JB013098.

Altamimi, Z., L. Metivier, P. Rebischung, H. Rouby, X. Collilieux; ITRF2014 plate motion model, *Geophysical Journal International, Volume 209*, Issue 3, 1 June 2017, Pages 1906-1912, https://doi.org/10.1093/gji/ggx147